RAPID COMMUNICATIONS

PHYSICAL REVIEW B VOLUME 50, NUMBER 11 15 SEPTEMBER 1994-I

Experimental characterization of electron trajectories in antidot lattices

R. Schuster, G. Ernst, K. Ensslin, and M. Entin*
Sektion Physik, Ludwig-Maximilians-Universität München, Geschwister Scholl Platz 1, D-80539 München, Germany

M. Holland
Department of Electronics, University of Glasgow, Glasgow G12 8QQ, United Kingdom

G. Böhm and W. Klein
Walter Schottky Institut, Technische Universität München, D-85748 Garching, Germany
(Received 23 May 1994)

The magnetic-field-dependent conductivity of a square antidot lattice is calculated from the experimentally determined magnetoresistance and Hall resistance. Close to the commensurability conditions where the magnetoresistance always displays pronounced maxima we find a crossover from minima to maxima in the conductivity as a function of antidot size. We interpret this behavior in terms of different classes of electron trajectories whose relative importance depends on the size of the antidots with respect to the lattice period.

Antidot lattices represent an ideal system to investigate the electronic properties of lateral superlattices.[1–5] So far, most experiments are dominated by classical effects that rely on the chaotic and regular trajectories arising in the antidot potential landscape.[6] Experimentally, pronounced maxima occur in the magnetoresistance at low magnetic fields where the classical cyclotron diameter fits around groups of antidots. In the same magnetic-field range the Hall effect displays plateaulike features and is even quenched or negative close to $B=0$.[4,7,8] Theoretically, the classical equations of motion have been solved in the presence of the antidot potential and the conductivity has been calculated using linear response theory.[6] The calculated conductivity has been converted to a resistivity and quantitative agreement has been found with the experimental data.

The quantum-mechanical band structure of an antidot lattice has been calculated by Silberbauer.[9] Using the Kubo formula he was also able to calculate the conductivity, convert it into a resistivity, and compare this resistivity with the experimental data.[10] Again the agreement with the experimental data is almost quantitative. The classical theory as well as the quantum-mechanical calculation average over a large ensemble of different electron trajectories or wave functions, respectively.

The fact that both the classical as well as the quantum-mechanical theory calculate the components of the conductivity tensor is purely based on technical reasons. Linear response describes the response to an externally applied voltage in terms of a conductivity. The experimentalists, on the other hand, measure resistances because this is the only way to make a well-defined four-terminal measurement. In the case of a Hall geometry whose dimensions are much larger than typical internal length scales of the system (elastic mean free path, phase coherence length, Fermi wavelength) the components of the resistivity tensor can be extracted in a straightforward manner from the measured resistances.

It is an experimental fact that in an antidot lattice a pronounced maximum occurs in the magnetoresistance when the classical cyclotron diameter matches the lattice period. The situation is not so clear for the higher-order commensurabilities and depends sensitively on the size of the antidots with respect to the lattice period.[4,6] In the present literature it is almost exclusively the magnetoresistance that is discussed experimentally as well as theoretically in terms of the position of the maxima. We want to show in this publication that the features that occur in the conductivity may be of equal importance and that a more comprehensive picture of classical electron trajectories can be obtained this way. In particular we argue that the occurrence of a maximum in the resistance cannot simply be identified with a pinned orbit.

The fabrication of our samples starts from a high-mobility two-dimensional electron gas (2DEG) based on the $Al_xGa_{1-x}As/GaAs$ material system. The pattern was defined by electron beam lithography and transferred onto the electron gas by a carefully tuned wet etching step. The details of this fabrication as well as the experimental setup are described in Ref. 11. However, the fabrication process is of minor importance and we believe that our analysis will lead to the same basic results if performed on magnetoresistance traces as obtained on samples fabricated by other technological means. All experimental data presented in this paper are obtained at $T=4.2$ K.

Figure 1(a) presents the experimentally determined magnetoresistance ρ_{xx} (solid line) as well as Hall resistance ρ_{xy} (dotted line) of an antidot lattice with period $p=480$ nm. The high-field Shubnikov–de Haas (SdH) oscillations are perfectly periodic in $1/B$ and facilitate the precise determination of the carrier density N_s of the 2DEG. The magnetic field B_c at which the classical cyclotron diameter matches the lattice period p is given by $B_c = 2\hbar\sqrt{2\pi N_s}/ep$, where $\hbar$ is Planck's constant and e is the quantum of the electric charge. This position of the magnetic field B_c is indicated by the vertical straight line in Fig. 1(a). The position of the maximum in ρ_{xx} lies very close to this value of B. The respective components of the conductivity tensor are calculated with the standard formulas for square geometries of the superlattice $\sigma_{xx} = \rho_{xx}/(\rho_{xx}^2 + \rho_{xy}^2)$, $\sigma_{xy} = \rho_{xy}/(\rho_{xx}^2 + \rho_{xy}^2)$. The experimental conductivities that are obtained in this way are presented in Fig. 1(b). In order to obtain a better understanding of the σ traces a series of curves for different gate volt-

0163-1829/94/50(11)/8090(4)/$06.00

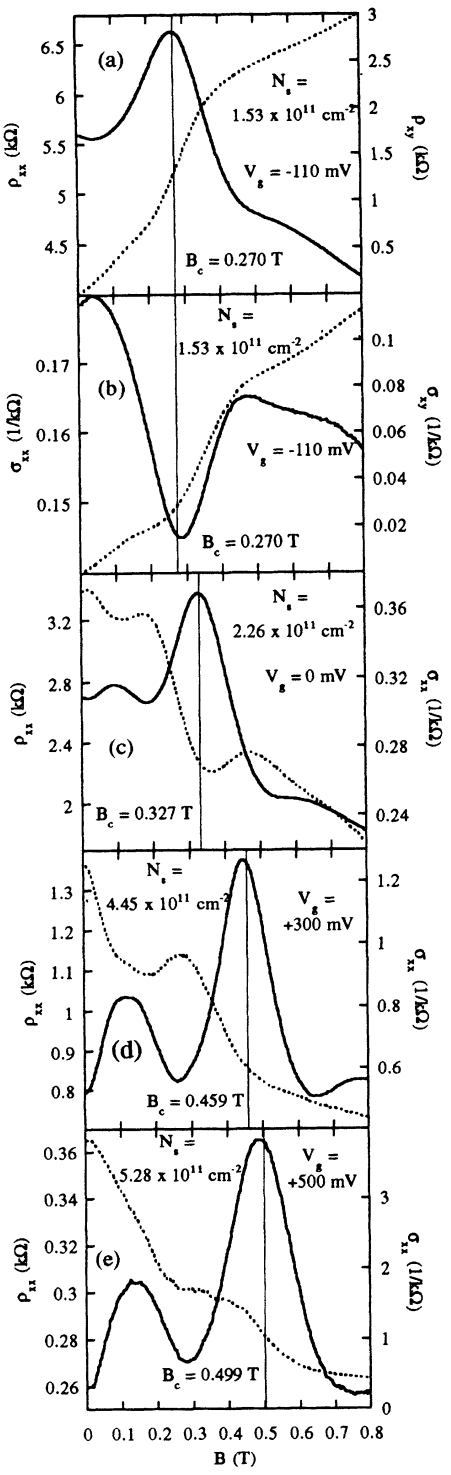

FIG. 1. (a) Magnetoresistance ρ_{xx} (solid line) and Hall resistance ρ_{xy} (dotted line) as a function of magnetic field for a gate voltage of $V_g = -110$ mV. The magnetic field B_c where the classical cyclotron diameter exactly matches the lattice period is marked by the vertical line. (b) Magnetoconductivity σ_{xx} (solid line) and Hall conductivity σ_{xy} (dotted line) as calculated from the data in (a) using the formulas given in the text. (c)–(e) Magnetoresistance ρ_{xx} (solid line, right-hand side) and magnetoconductivity σ_{xx} (dotted line, right-hand side) for several gate voltages $V_g = 0$, +300, and +500 mV. The position of the magnetic field B_c where the classical cyclotron diameter matches the lattice period is marked by the vertical line. The scale for the solid lines is on the left-hand side, the scale for the dotted lines on the right-hand side of the respective part of the figure.

ages is presented in Fig. 1. In 1(c)–1(e) the solid lines represent the magnetoresistance ρ_{xx}, the dotted lines the magnetoconductivity σ_{xx}. It is obvious especially for the higher carrier densities in Fig. 1 that the features that are related to commensurabilities are much less pronounced in the conductivities compared to the resistivities. This is related to the overall behavior of the two quantities in the classical limit. The magnetoresistance of a homogeneous electron gas in the classical limit is constant and given by $\rho_{xx} = 1/eN_s\mu$ where μ is the Drude mobility of the electron gas. In the case of an antidot lattice the commensurability oscillations are superimposed onto a horizontal line and therefore well discernible. In contrast the conductivity in the Drude limit is given by $\sigma_{xx} = eN_s\mu/(1 + \mu^2B^2)$ and therefore has an explicit B dependence. Any structure that might be superimposed on the overall $\sigma_{xx}(B)$ curve is hard to discern from the strong monotonic decay of σ_{xx} as a function of increasing B. Furthermore the position of a maximum or a minimum may be shifted because of the pronounced background curve. This is again obvious in the data as presented in Fig. 1.

The straight vertical lines in Fig. 1 mark the magnetic field B_c as defined above. Again it is obvious that the highest lying maximum in ρ_{xx} is clearly positioned at B_c within the experimental accuracy. For larger Fermi energies, i.e., increased carrier densities, the elastic mean free path increases and a second maximum occurs in ρ_{xx} for lower B values.

The behavior of σ_{xx}, on the other hand, is quite different. For low carrier densities [Fig. 1(b)] there is a pronounced minimum in σ_{xx} almost exactly where ρ_{xx} displays a maximum. For increasing carrier density, 1(c)–1(e), this minimum becomes less pronounced and shifts to higher fields. Simultaneously a second minimum occurs at about the magnetic-field position where the low-field maximum in ρ_{xx} arises, 1(d). For high carrier densities, finally, the high-field minimum in σ_{xx} has almost completely disappeared and a maximum occurs in σ_{xx} at a magnetic field slightly below B_c. It is clear that the oscillatory structure in σ_{xx} differs dramatically from the one in ρ_{xx}.

In the following we will give an interpretation of this data based on characteristic electron trajectories in the system. For smooth potentials Fleischmann, Geisel, and Ketzmerick[6] found that electrons on pinned electron trajectories occupy a finite volume in phase space. The question arises as to what effect this has on the conductivity or the resistivity of the system. The Einstein relation connects the diffusion coefficient to the conductivity of the system. Consequently we expect the diffusion of the electrons to be reduced if pinned electron orbits exist. This is in agreement with theoretical calculations that consider the influence of a pinned electron orbit on the conductivity[12] as well as with the experimental observation in Fig. 1(b). It is very difficult, however, to establish the influence of a given type of electron trajectory on the resistivity of the system.[12]

Baskin *et al.*[13] have calculated the electron trajectories in an antidot lattice with hard walls. For $2R_c = P$ they find an enhanced diffusion coefficient and therefore maxima in the conductivity for so-called runaway trajectories that bounce off neighboring antidots and therefore channel between the rows of antidots. This situation is similar to the experimental data as presented in Fig. 1(e) where the features in σ_{xx} are

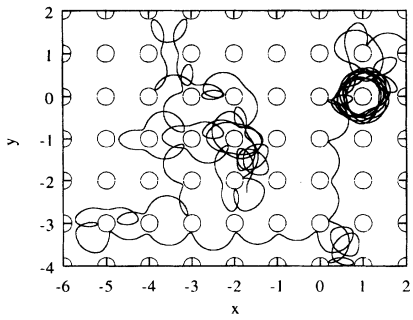

FIG. 2. The circles mark the equipotential lines where the antidot potentials penetrate the Fermi energy. The electron trajectory is calculated using the classical equations of motion with the potential as given in the text. The size of an antidot at the Fermi energy is chosen to be 0.4 of the lattice period. The magnetic field is such that the condition $2R_c=p$ is fulfilled. At the upper right a typical pinned electron orbit occurs. On the bottom of the figure an electron travels along six lattice periods in terms of a quasirunaway trajectory.

only weakly pronounced but a clear maximum arises in ρ_{xx} at a magnetic field just below the commensurability condition $2R_c=p$. Apparently in a typical antidot potential electrons on chaotic paths follow runaway as well as pinned trajectories for some time. This leads to quasipinned[6] as well as quasirunaway trajectories. We use this terminology in line with the original literature.[13]

In Fig. 2 we present a typical electron trajectory calculated for a potential $V(x,y)=V_0\cos^4(\pi x)\cos^4(\pi y)$ where the circles show the equipotential lines $V(x,y)=E_F$. The magnetic field is chosen such that $2R_c=p$. It is obvious that along the trajectory there are regions where the electron channels between the rows of antidots and other regions where it orbits around a single antidot. The smaller the antidots and the harder the potential walls, the more likely it is that quasirunaway trajectories exist. For very large antidots or very smooth potential walls the pinned orbits are thought to dominate the trajectories.

A very similar trajectory is presented in Fig. 8 of Ref. 7. There the electron channels along the diagonal of the square for some length of the trajectory while it predominantly encircles single antidots for the rest of its path.

This scenario is in agreement with the picture that evolves from Fig. 1. For low carrier densities the antidots will be rather large and the potential walls are smooth. Consequently, the electrons tend to encircle single antidots and the conductivity displays a minimum. Since the magnetoresistance is much larger than the Hall resistance $\rho_{xx}>\rho_{xy}$ it follows from the above relations that $\rho_{xx}\propto 1/\sigma_{xx}$. Consequently we expect a maximum in ρ_{xx} as observed in Fig. 1(a). For increasing gate voltage the carrier density and therefore the Fermi energy rises. This leads to smaller antidots and steeper potential walls as caused by the improved screening behavior of the electron gas. Experimentally this development is displayed through Figs. 1(a)–1(e). The minimum [Fig. 1(b)] in σ_{xx} gradually turns into a maximum [Fig. 1(e)]. Simultaneously the overall resistance decreases and we are now in a situation where $\rho_{xx}<\rho_{xy}$. The maximum in ρ_{xx} corresponds to a shoulder in σ_{xx}. In this kind of potential landscape we expect that the conductivity is not dominated by pinned orbits but rather it is strongly influenced by runaway trajectories in agreement with the experimental findings.

The arguments as given above hold for the fundamental commensurability $2R_c=p$ where the electrons classically encircle a single antidot. For larger cyclotron diameters, i.e., smaller magnetic fields, runaway trajectories are extremely unlikely to occur. We expect that in this case pinned electron orbits represent the favorable trajectories. We anticipate that minima will occur in the conductivity as can be seen in the experimental data in Figs. 1(d) at $B\approx 0.1$ T. In order to check this conjecture in more detail we fabricated an antidot lattice with the same lattice period and a smaller distance (27 nm) of the 2DEG to the surface. This facilitates the fabrication of smaller antidots and consequently more features in the magnetoresistance spectra.

Figure 3(a) presents the Hall resistance as well as the magnetoresistance for such a sample where we estimate the diameter of the antidots at the Fermi energy to be about 20% of the lattice period. In addition to the pronounced maximum in ρ_{xx} that occurs at the commensurability condition a series of low-field maxima appear. The respective conductivities σ_{xx} and σ_{xy} are displayed in Fig. 3(b). The features in σ_{xx} are superimposed on a pronounced background and hard to resolve in detail. In order to extract more information we made a fit to the σ_{xx} data assuming a Drude-like background with $\sigma_{xx}=P_1/(1+P_2B^2)$ where P_1 and P_2 are the fitting parameters. The results of this procedure are indicated by the dashed line in Fig. 3(b). The dotted line in 3(c) shows the normalized conductivity (difference between σ_{xx} and the fit) together with the results for ρ_{xx} (solid line). The details of the normalized conductivity do not depend critically on the fitting process. The straight vertical lines mark the magnetic-field positions where maxima occur in ρ_{xx}.

A pronounced maximum occurs in the normalized conductivity close to the commensurability condition $2R_c=p$ at $B\approx 0.35$ T. This structure can already clearly be identified as a maximum in the original conductivity as presented in Fig. 3(b). The calculated data for σ_{xx} by Silberbauer and Rössler[10] show a very similar behavior. For smaller magnetic fields where larger cyclotron orbits become important more features occur in the magnetoresistance ρ_{xx}. There are always features in the normalized conductivity that are closely related to the maxima in ρ_{xx}. However, for smaller magnetic fields these are clearly minima as indicated by the dash-dotted vertical lines. We conclude that for small magnetic fields maxima in ρ_{xx} are related to minima in σ_{xx} while for large magnetic fields maxima occur in both curves. This is again in agreement with the general picture as presented before. In this particular sample with very small antidots runaway trajectories are very likely to occur for cyclotron diameters comparable in size to the lattice period. This leads to an enhanced diffusion coefficient and consequently to a maximum in the conductivity. For smaller magnetic fields, however, runaway trajectories have to traverse many lattice periods and we expect the pinned orbits to take over which explains the observed minima in the normalized conductivity.

It is possible to assess theoretically the significance of a special kind of trajectory and its particular influence on the conductivity in contrast to the resistivity[12] in agreement with the arguments given above. The details of the experimental antidot potential at the Fermi energy are difficult to access. The extreme cases are, however, relatively clear. For an an-

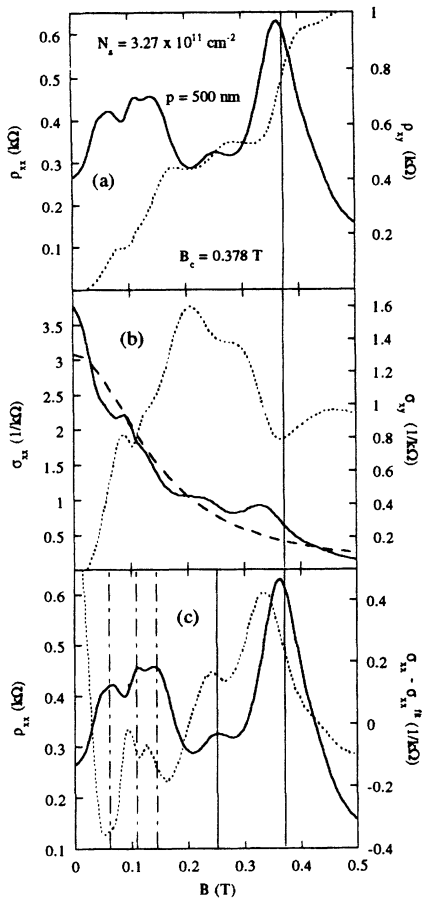

FIG. 3. Magnetoresistance and Hall resistance (a), magnetoconductivity and Hall conductivity (b), and magnetoresistance and normalized conductivity (c) for a sample with especially small antidots. The scale for the solid lines is on the left-hand side, the scale for the dotted lines on the right-hand side of the figure. The solid vertical line that goes through all three parts of the figure marks the magnetic field B_c, where the commensurability condition $2R_c=p$ is fulfilled. The dashed curve in (b) is a fit to the solid curve σ_{xx} by the formula given in the text. The normalized conductivity [dotted curve in (c)] is obtained from the subtraction of the fit curve to σ_{xx} from the real σ_{xx} curve as displayed in (b). The straight vertical lines in (c) mark the magnetic fields where maxima occur in ρ_{xx}. At the solid lines the normalized conductivity displays maxima, while at the positions of the dash-dotted lines it exhibits minima.

tidot lattice with large antidots runaway trajectories can hardly exist and we expect pinned orbits to give the important contribution to the commensurability oscillations. On the other hand, if the antidots are very small the potential between the antidots is fairly flat and the electrons will follow almost unperturbed cyclotron orbits. However, runaway trajectories can exist even down to very small antidots with very steep walls.

These arguments follow from experimental observations but are not bound to our particular set of samples. Very similar conductivity data can be obtained from other experimental data as well as from the calculations. The experiments as well as the classical and quantum-mechanical observations on antidot superlattices from other authors also fall within this general picture. We think, however, that our interpretation combines two extreme theoretical points of view and enriches the interpretation of magnetotransport data on antidot lattices. In particular we conclude that the standard picture that maxima in the magnetoresistance can simply be identified with pinned electron orbits has to be modified and extended.

We have presented a selection of experimentally determined magnetotransport traces as obtained on square antidot lattices. While the general features of the components of both the conductivity as well as the resistivity tensors can be reproduced nicely by classical and quantum-mechanical calculations our interpretation of various characteristic electron trajectories emphasizes the importance of the antidot potential landscape. We argue that for large antidots pinned electron orbits around groups of antidots are dominant leading to maxima in the conductivity. For very small antidots so-called runaway trajectories become important and the electrons channeling through the rows of antidots conceivably lead to an enhanced diffusion and therefore an enhanced conductivity. All of these effects result in pronounced maxima in the magnetoresistance independent on the details of the system. The usual simple identification of a maximum in the magnetoresistance with a pinned electron orbit has to be modified. In addition the question of whether the conductivity or the resistivity contains the fundamental physics has to be asked anew. We believe, however, that the analysis of the conductivity can give more physical insight in the present case.

We are indebted to R. Ketzmerick for an exchange of ideas and for access to his data prior to publication. It is a pleasure to thank R. Fleischmann, A. Lorke, J. P. Kotthaus, U. Rößler, T. Schlösser, S. Ulloa, D. Weiss, and D. Wharam for most valuable discussions. We are grateful to the Deutsche Forschungsgemeinschaft and the ESPRIT Basic Research Action for financial support.

*Permanent address: Institute of Semiconductor Physics, Siberian Branch of the Russian Academy of Sciences, 630090 Novosibirsk, Russia.

[1] H. Fang *et al.*, Appl. Phys. Lett. **55**, 1433 (1989).
[2] K. Ensslin and P. M. Petroff, Phys. Rev. B **41**, 12 307 (1990).
[3] A. Lorke *et al.*, Superlatt. Microstruct. **9**, 103 (1991).
[4] D. Weiss *et al.*, Phys. Rev. Lett. **66**, 2790 (1991).
[5] G. M. Gusev *et al.*, Pis'ma Zh. Eksp. Teor. Fiz. **54**, 369 (1991) [JETP Lett. **54**, 364 (1991)].
[6] R. Fleischmann *et al.*, Phys. Rev. Lett. **68**, 1367 (1992).
[7] For a review see D. Weiss *et al.*, Surf. Sci. **305**, 408 (1994).
[8] For a review see R. Schuster and K. Ensslin, Festkörperprobleme (to be published).
[9] H. Silberbauer, J. Phys. C **4**, 7355 (1992).
[10] H. Silberbauer and U. Rössler (unpublished).
[11] R. Schuster *et al.*, Phys. Rev. B **49**, 8510 (1994); K. Ensslin and R. Schuster, in III-V Semiconductor Quantum Systems, edited by K. Ploog (Institution of Electrical Engineers, New York, in press).
[12] R. Ketzmerick (private communication).
[13] E. M. Baskin *et al.*, Pis'ma Zh. Eksp. Teor. Fiz. **55**, 649 (1992) [JETP Lett. **55**, 679 (1992)].